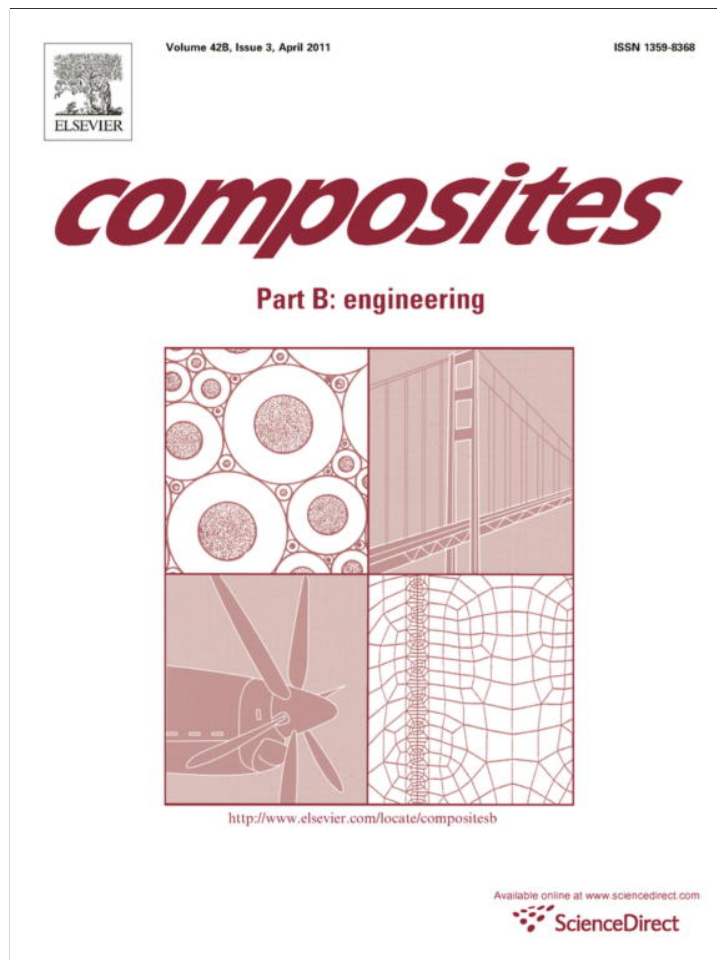


Provided for non-commercial research and education use.  
Not for reproduction, distribution or commercial use.



This article appeared in a journal published by Elsevier. The attached copy is furnished to the author for internal non-commercial research and education use, including for instruction at the authors institution and sharing with colleagues.

Other uses, including reproduction and distribution, or selling or licensing copies, or posting to personal, institutional or third party websites are prohibited.

In most cases authors are permitted to post their version of the article (e.g. in Word or Tex form) to their personal website or institutional repository. Authors requiring further information regarding Elsevier's archiving and manuscript policies are encouraged to visit:

<http://www.elsevier.com/copyright>



Contents lists available at ScienceDirect

## Composites: Part B

journal homepage: [www.elsevier.com/locate/compositesb](http://www.elsevier.com/locate/compositesb)

# In situ synthesis of polyoxadiazoles (POD) and carbon black (CB) as an approach to POD/CB nanocomposites

Marcio R. Loos<sup>a,\*</sup>, Volker Abetz<sup>a</sup>, Karl Schulte<sup>b</sup>

<sup>a</sup>Institute of Polymer Research, GKSS-Forschungszentrum Geesthacht GmbH, Max-Planck-Str. 1, 21502 Geesthacht, Germany

<sup>b</sup>Institute of Polymer & Composites, Hamburg University of Technology, Denickestrasse 15, 21073 Hamburg, Germany

## ARTICLE INFO

## Article history:

Received 23 July 2010

Received in revised form 20 September 2010

Accepted 10 December 2010

Available online 8 January 2011

## Keywords:

A. Nano-structures

A. Polymer-matrix composites (PMCs)

B. High-temperature properties

B. Mechanical properties

Polyoxadiazoles

## ABSTRACT

Pristine carbon black was oxidized with poly(phosphoric acid) to produce carboxyl groups. The carboxyl groups were consecutively treated with hydrazine sulfate to introduce arylcarbonyl and CONHNH<sub>2</sub> groups. The groups on the CB surface were reacted with dicarboxylic acid to anchor the growing of polyoxadiazole chains. The properties of the bulk POD/CB composites were characterized by elemental analysis (EA), Fourier transform infrared (FTIR) and thermogravimetric analysis (TGA). The final composites were processed in films using a solution method aided by the use of a mini-calendar for final high shear mixing. Transmission electron microscopy (TEM), atomic force microscopy (AFM), dynamic mechanical thermal analysis (DMTA) and tensile tests were used to systemically characterize the high performance composite films. The POD composites with high molecular weight (in the order of magnitude of 10<sup>5</sup> g/mol) were soluble in polar aprotic solvents and stable at temperatures as high as 465 °C. The incorporation of the CB enhanced the overall mechanical properties of the composites at low CB content due to the presence of strong interfacial interaction between the polymer matrix and the filler.

© 2011 Elsevier Ltd. All rights reserved.

## 1. Introduction

Nanocomposites are a class of composites in which the dimensions of the reinforcement phase are in the range of 1–100 nm. Because of their nanometer size characteristics, nanocomposites possess superior properties to more conventional composites reinforced with micro-sized fillers [1–3].

The development of high performance/high temperature polymers has been a demand from the aerospace industries seeking for new materials. Synthesis of polymers containing oxadiazole rings was part of a NASA program on high performance/high temperature polymer for potential use as coatings and composite matrices on aerospace vehicles [4,5]. Particularly, polyoxadiazole (POD) thermoplastic polymers have a great potential as structural material because of their superior thermal, chemical and mechanical properties [6]. POD fibers present a combination of properties (such as good strength and stiffness, good fatigue resistance and low density) that makes these fibers competitive in performance when compared to other reinforcing agents, such as glass, steel, and commercial high temperature fibers (Kevlar, X-500, Cermel, Nomex) [6–8]. Technological applications have also been reported in connection with the basic nitrogen atoms and aromatic

character of the oxadiazole heterocyclic ring [9], enabling their use as emissive layers in light-emitting diodes [10–12], electron/proton conducting materials [13,14], electrochemical/acid sensors [15,16], and materials to prevent metal corrosion [17,18].

Recent applications of fiber reinforced polymers in aircraft propulsion systems have resulted in substantial reductions in both engine weight and manufacturing costs [19,20]. A major effort underway in this area is the development of high temperature reinforced polymers, usable up to temperatures as high as 425 °C [21,22]. Continued improvements in the stability of polymer matrices coupled with improvements in polymer/filler interfaces, composite processing, and oxidation-resistant coatings will yield reinforced polymers for use at high temperatures [21,23,24]. In this context, the reinforcement of POD polymer with nanofillers offer a possibility to obtain new light-weight materials suitable to high performance/high temperature applications.

Carbon-based nano-structured fillers include single-walled carbon nanotubes (SWCNTs), multi-walled carbon nanotubes (MWCNTs), carbon nanofibers (CNFs) and carbon black (CB) and they have attracted great attention due to their unique properties for a wide variety of potential applications such as nanocomposites, electronic devices, field emission display, hydrogen storage, and other fields of materials science [25,26]. When they are used as reinforcing additives for nanocomposites, they could deliver their outstanding properties to support matrices such as polymers [27–33], ceramics [34,35], and even low melting metals [36,37]. The resultant nanocomposites would possibly possess enhanced

\* Corresponding author. Present address: Department of Macromolecular Science and Engineering, Case Western Reserve University, Cleveland, OH 44106, USA. Tel.: +1 216 368 1895; fax: +1 216 368 4202.

E-mail address: [marcio.loos@case.edu](mailto:marcio.loos@case.edu) (M.R. Loos).

properties providing various potential applications for areas, which require affordable, light-weight and multifunctional materials.

Major problem is the difficult in dispersion of carbon-based fillers in a polymer matrix due to its strong van der Waals interactions. Another issue is the weak interfacial interaction between filler and polymer. The chemical modification is one of the most important approaches to overcome these problems [38,39]. Generally it arises from the functional groups on the surface of the filler, which are derived by the oxidation processes. Other approaches, including the direct dispersion of fillers in the polymer solution via sonication [40–42], surfactant assisted processing of filler-polymer composites [43,44], and in situ polymerization in the presence of the fillers [45,46], have been proposed for obtain polymer composites with homogeneously dispersed fillers.

Compared with carbon-based nano-structured materials as SWCNTs, MWCNTs, CNFs and fullerenes, carbon black nanoparticle is a relatively conductive carbon material composed of 90%–99% elemental carbon, more readily available, and has been widely applied in the industry because of its low price.

In this paper, we demonstrate a fast direct method to obtain POD/CB composites where the CB is in situ functionalized during the synthesis of poly(1,3,4-oxadiazoles) using poly(phosphoric acid) (PPA) as a condensing agent. PPA is a moderate acidic medium and promotes disaggregation to help homogeneous dispersion and purification of CB without or with little damages. Because of the different reactivity of monomers, significant lower synthesis time is required (4 h) to produce the composite polyoxadiazole compared to other composite polymers synthesized via in situ polymerization in PPA [47–50].

## 2. Experimental

### 2.1. Materials

All the reagents and solvents were purchased from Aldrich Chemical and used as received. Dicarboxylic acid 4,4'-diphenylether, DPE (99%), dimethyl sulfoxide, DMSO (>99%), hydrazine sulfate, HS (>99%), sodium hydroxide, NaOH (99%), poly(phosphoric acid), PPA (115% H<sub>3</sub>PO<sub>4</sub>), carbon black (CB, Average particle size: 18 nm, SSA: >250 m<sup>2</sup>/g, Evonik/Degussa).

### 2.2. Instrumentation

Elemental analysis was conducted on a Carlo Erba Elemental Analyzer-Mod 1108. Infrared spectra were recorded on a Bruker Equinox IFS 55 spectrophotometer in the range 4000–400 cm<sup>-1</sup>. TEM images were obtained using a Tecnai G2 F20 field emission transmission electron microscopy at an acceleration voltage of 200 kV; the samples were cut into slices of 80 nm thickness using a ultracut microtome with diamond knife. Atomic force microscopy of samples was done by using a multi mode scanning probe microscope model with a nanoscope IV controller by Digital Instruments Inc. (Veeco Metrology Group). AFM observations were carried out in air at ambient conditions (25 °C) using tapping mode probes with constant amplitude. Micrographs in topographic and phase contrast modes were obtained. A Viscotek SEC apparatus equipped with Eurogel columns SEC 10.000 and PSS Gram 100, 1000, with serial numbers HC286 and 1515161 and size 8 × 300 mm was employed to evaluate the weight average molecular weights of polymer and nanocomposite samples. The equipment was calibrated using polystyrene standards (Merck) with weight average molecular weights ranging from 309 to 9,44,000 g/mol. A solution with 0.05 M lithium bromide in dimethylacetamide, DMAc (≥99.9%, Aldrich) was used as the carrier. Thermogravimetric analysis experiments were carried out in a Netzsch 209 TG, equipped with a TASC 414/3 thermal

analysis controller. The bulk sample, under argon and air atmosphere, was heated from 100 °C to 900 °C at 10 °C/min. Dynamic mechanical thermal analysis was performed using a TA instrument RSA 2 with a film tension mode at a frequency of 1 Hz and 0.1 N initial static force. The temperature was varied from 25 °C to 500 °C at a heating rate of 2 °C/min and at a constant strain of 0.05%. Tensile tests were performed according to the ASTM D882-00 using a Zwick-Roell equipment with a 500 N load cell. The reported values correspond to an average of at least eight specimens.

### 2.3. Representative synthesis of sulfonated poly(1,3,4-oxadiazoles) with 0.1 wt.% CB load

The reaction condition for the synthesis of the POD was selected based on the previous studies [51]. Reactions were carried out in a 250 ml three-necked flask equipped with a dry nitrogen inlet tube, to keep the reaction atmosphere free of oxygen and water. Initially PPA, and carbon black (0.02 g), was added to the flask and heated up to 80 °C under sonication and simultaneous mechanical stirring during 1 h. Afterwards HS (0.031 mol) and DPE (0.013 mol) was added to the mixture and reacted under mechanical stirring at 160 °C during 4 h. At the end of the reaction, the final solution was precipitated in the form of stable fibers into water containing 5% w/v of NaOH. The final polymer yield was always close to 100% in respect to the limiting reactant.

### 2.4. Fabrication of the POD/CB films

To study the physical properties and morphology of the resultant composites, films were fabricated using a calander (model EX-AKT 80E). Solutions with a polymer concentration of 10 wt.% were prepared in DMSO. The solution was magnetically stirred at 60 °C during 3 h. Afterwards the suspension was added to a mini-calander for final high shear mixing. The gap size between the rolls was 5 μm (1st roll), 10 μm (2nd roll) and the speed was set to 50 rpm. The suspension was then collected and re-dissolved in DMSO under stirrer at 60 °C during 3 h. Homogeneous films were cast in glass plates. After casting, the DMSO was evaporated in a vacuum oven at 90 °C for 24 h. For further residual solvent removal, the membranes were immersed in water bath at 50 °C for 24 h and dried in a vacuum oven at 90 °C for 24 h. The final thickness of the films was about 60 μm.

## 3. Results and discussion

### 3.1. Synthesis of POD/CB composites

In situ polymerization is one of the most viable routes to prepare nanocomposites. Sulfonated polyoxadiazole composites containing different concentrations of carbon black (0.1, 0.5 and 1.0 wt.%) were successfully prepared via in situ polymerization. The proposed covalent functionalization of the CB is schematically shown in Fig. 1. Covalent attachment of POD onto the CB surfaces should be expected to occur by condensation reaction of COOH groups generated in situ on the surface of the CB with the NH<sub>2</sub>NH<sub>2</sub> hydrazine monomer, leading to the formation of arylcarbonyl and CONHNH<sub>2</sub>, respectively. The growing POD chains on the CB surface is expected to promote the physical contact with the polymer matrix allowing an efficient load transfer from the reinforcement phase to the matrix phase in the nanocomposites.

During the synthesis, the initial color of all reaction mixtures was black because of the CB dispersion (Fig. 2a). On all cases, the reaction mixtures were homogeneous with drastic increase in viscosity. The viscosity had reached the point that the dope stuck to the stirring rod, and this provided a visual signal that high

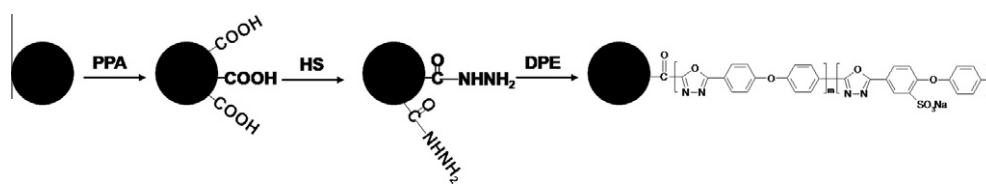


Fig. 1. Proposed route for the oxidation of the CB represented as a black circle and grafting of POD on its surface.

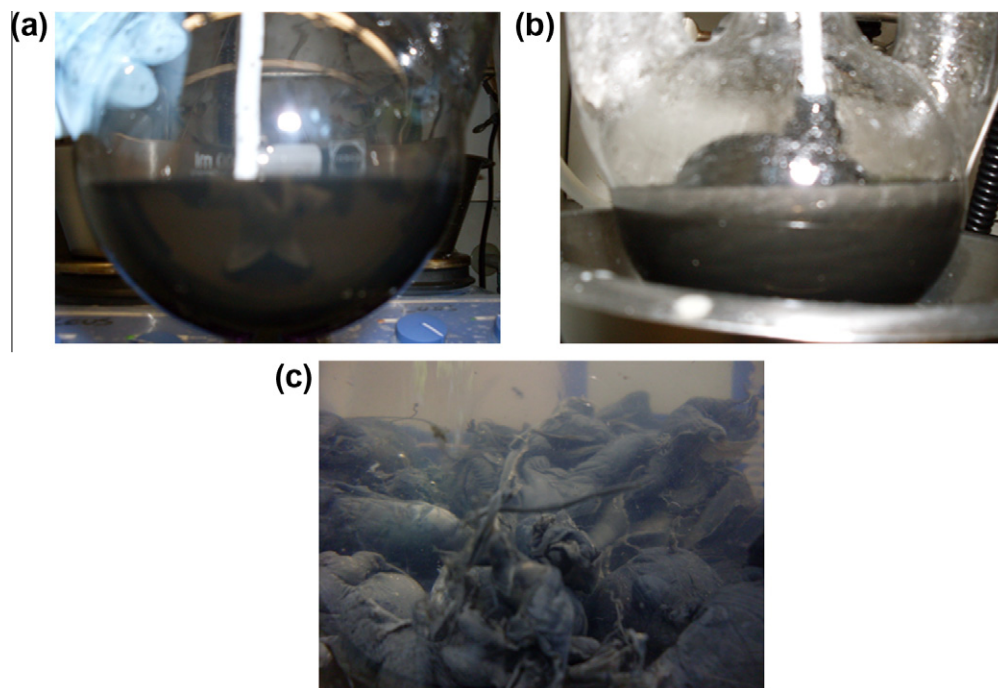


Fig. 2. Digital photographs of the reaction mixture: (a) after the pre-dispersion step, (b) 3 h after starting of the synthesis, and (c) composite precipitated like “noodles”.

molecular weight polymers were being synthesized (Fig. 2b). At the end of the synthesis the viscosity was even higher, then water was added into the reaction vessel and big chunk of product was isolated (Fig. 2c).

Elemental analysis data for the sulfonated polyoxadiazole nanocomposites shown in Table 1 are in agreement with the value range for the sulfonated polyoxadiazoles. The polyoxadiazole sulfonation reaction, which occurs during the synthesis due to the presence of sulfuric acid in the solution of hydrazine sulfate has been recently recognized and characterized by Gomes et al. [13]. The polyoxadiazole sulfonation level (S/C) has been shown to be dependent on the reaction time [14], reaching the value range 0.085–0.0998 (44%–51%) for the synthesis performed in 4 h. In this study the sulfonation level has changed for all the used contents of CB (Table 1). The presence of CB causes a decrease of up to 15% in the sulfonation level of nanocomposites reinforced with 0.1–0.5 wt.% and an increase of 19% to the composites reinforced with

1.0 wt.%. An additional factor could be the homogeneity differences of CB concentration in the reaction medium. In regions where the CB concentration is overall or much better distributed, the sulfonation level should proportionally decrease [52]. This explains the lower sulfonation level obtained for the concentrations of 0.1 and 0.5 wt.% CB.

High molecular weights ranging from 2.9 to  $3.3 \times 10^5$  g/mol with a polydispersity between 2.4 and 4.0 for the CB-based composites were obtained (Table 1). Therefore, the addition of CB implies in a decrease in molecular weight and increase in polydispersity. The observed changes in molecular weight, polydispersity and sulfonation level can be explained by the presence of the CB in the reaction medium, which may influence the synthesis chemically as well as physically. Therefore, the comparison of the composites with the neat sulfonated polyoxadiazole is difficult once the polymer shows different sulfonation levels (S/C), which influence the dipole–dipole interactions between the sulfonated groups

Table 1  
Elemental analysis data, average molecular weight and polydispersity (PDI), for the sulfonated polyoxadiazole nanocomposites.

CB (wt.%)	S/C		N/C		SL (%) <sup>a</sup>	M <sub>w</sub> (g/mol)	PDI
	Calc.	Found	Calc.	Found			
0	0.099	0.091	0.17	0.17	48	$4.2 \times 10^5 \pm 3 \times 10^3$	2.0 ± 0.1
0.1	0.099	0.080	0.17	0.17	41	$3.1 \times 10^5 \pm 6 \times 10^3$	4.0 ± 0.2
0.5	0.099	0.083	0.17	0.16	43	$2.9 \times 10^5 \pm 3 \times 10^3$	2.4 ± 0.3
1.0	0.10	0.11	0.17	0.17	57	$3.3 \times 10^5 \pm 6 \times 10^3$	2.8 ± 0.4

<sup>a</sup> Sulfonation level assuming 100% sulfonated when  $m = 0$  (S/C = 0.19).

[51,52]. The introduction of sulfonic groups increases the intermolecular interaction and consequently increases the  $T_g$  and mechanical properties [51].

Fig. 3 shows the appearance of the POD/CB composites. The composites films were placed on a paper printed with the words 'GKSS Research Centre – Institute of Polymer Research, Hamburg University of Technology – TUHH'. The composites become darker in color with increasing of CB content. Samples with CB concentration of 0.1 wt.% possess good optical clarity.

In order to confirm the covalent attachment proposed in Fig. 1, FTIR analysis of the composites were performed. Fig. 4 shows the representative FTIR spectra of neat sulfonated polyoxadiazole, composites and CB. There were no discernable characteristics among samples. Assignments are observed for the pristine polymer at 1603 and 1490  $\text{cm}^{-1}$  arising from C=C stretching of the aromatic groups and the assignments placed at 1468  $\text{cm}^{-1}$  and 1416  $\text{cm}^{-1}$  related to the C=N stretching of oxadiazole ring group [30]. The infrared analysis was also performed on the CB. The two bands at 1690 and 1522  $\text{cm}^{-1}$  can be attributed to stretching vibrations of C=O and C=C groups in the carbon material [53].

### 3.2. Solution properties

The nanocomposites reinforced with different amounts of CB were highly soluble in polar aprotic solvents such as DMSO, *N*-methyl-2-pyrrolidone (NMP), *N,N*-dimethylacetamide (DMA) and *N,N*-dimethylformamide (DMF). Such solubility allow the further processing of the nanocomposites using the solvent casting technology [54] and the spinning of fibers with potential properties to be used as reinforcing agent in polymer–matrix composites.

### 3.3. Dynamic mechanical thermal analysis of the POD/CB composites

Fig. 5 shows the DMTA curves of the neat POD and its composites. The values of  $E'$ , which are correlated with the elastic modulus



Fig. 3. Digital photographs of POD nanocomposites reinforced with different CB amounts.

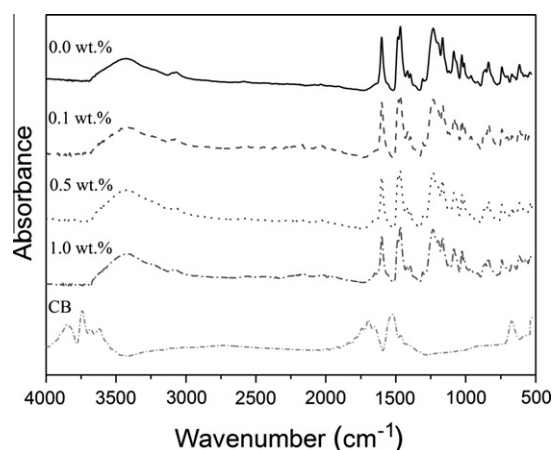


Fig. 4. Representative FTIR spectra of the neat polyoxadiazole, pristine CB and CB/POD composites.

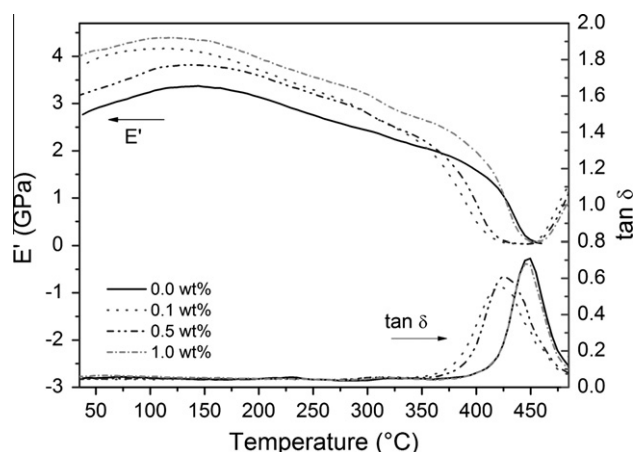


Fig. 5. (a) variation of the storage modulus ( $E'$ ) and  $\tan \delta$  as a function of temperature for the CB/POD nanocomposites.

of the material, for the neat POD and the POD/CB composites containing 0.1, 0.5 and 1.0 wt.% CB at 100 °C are 3.18, 4.16, 3.70 and 3.92 GPa, respectively. The use of only 0.1 wt.% CB increases  $E'$  up to 31% at this temperature. It can be still seen that even at 300 °C the nanocomposites maintain a high stiffness. The increase of  $E'$  observed in the composites with 0.1–0.5 wt.% CB, despite the lower sulfonation level and molecular weight in comparison to the neat POD, reflects the interaction between the CB and the POD [55,56], and the homogeneous dispersion.

The variation of  $\tan \delta$  among various CB contents is also plotted against temperature in Fig. 5 and values of the  $T_g$  are listed in Table 2. The  $T_g$  values of the composites are affected by the sulfonation level, molecular weight ( $M_w$ ), polydispersity and by the CB content. Considering the  $T_g$  value obtained from the peak of  $\tan \delta$  as a function of temperature (Fig. 5), it can be seen that the  $T_g$  decrease up to 22 °C with the addition of 0.5 wt.% CB. When the filler is homogeneously distributed in a polymeric matrix, the  $T_g$  of the composites should increase with filler content [52]. Such decreased observed here in  $T_g$  values might be attributed mainly to the variation of the sulfonation level and molecular weight. Comparing Tables 1 and 2, one can see that the composite with the lower  $T_g$  (0.1–0.5 wt.% CB) has a lower  $M_w$  and sulfonation level that those of the neat polyoxadiazole. Therefore, even with a homogeneous dispersion and good interaction between filler and matrix phase, as confirmed by morphological characterization, the  $T_g$  decrease. However, nanocomposites reinforced with 1.0 wt.% CB have not shown changes in the  $T_g$  value. Such result is attributed to the increase observed in sulfonation level and polydispersity allied with the decrease on molecular weight, as discussed previously. As depicted in Fig. 5, the value of  $\tan \delta$  decreased from 0.71 to 0.56 when 0.1 wt.% CB was added to the POD matrix. The interaction between the CB and the polyoxadiazole matrix reduce the free volume in the nanocomposites, make then behave more elastically, thus leading to the observed decrease in the intensity of  $\tan \delta$  peak [57–59]. As expected, composites with 1.0 wt.% CB do not show significant changes in the value of  $\tan \delta$ . This result further indicates that the CB reinforces the POD matrix by virtue of their good dispersion and interaction.

### 3.4. Thermal analysis of the POD/CB composites

In order to study the thermal stability of the composites, TGA characterization has been carried out under dry air and argon atmospheres. The results are depicted in Table 2. Overall, the thermal stabilities of nanocomposites in argon were unchanged as

**Table 2**  
Glass transition temperature, thermal stability and tensile properties of the CB/POD nanocomposites.

CB (wt.%)	$T_g$ (°C) <sup>a</sup>	$T_{d5}$ (°C) <sup>b</sup>		Char at 700 °C (%)		$E$ (MPa)	$\sigma_M$ (MPa)	$\varepsilon$ (%)
		In arg.	In air	In arg.	In air			
0.0	447	466	469	59	14	2690 ± 42	153 ± 8	45.7 ± 6.8
0.1	425	463	467	57	52	2840 ± 100	118 ± 8	21.5 ± 4.0
0.5	425	465	463	57	9	2680 ± 84	161 ± 7	59.0 ± 5.4
1.0	445	468	469	59	18	2270 ± 130	109 ± 7	34.5 ± 1.0

$E$ : Young modulus;  $\sigma_M$ : tensile strength;  $\varepsilon$ : elongation at break.

<sup>a</sup> Glass transition temperature measured by DMTA ( $\tan \delta$ ).

<sup>b</sup> 5% weight loss temperature measured by TGA.

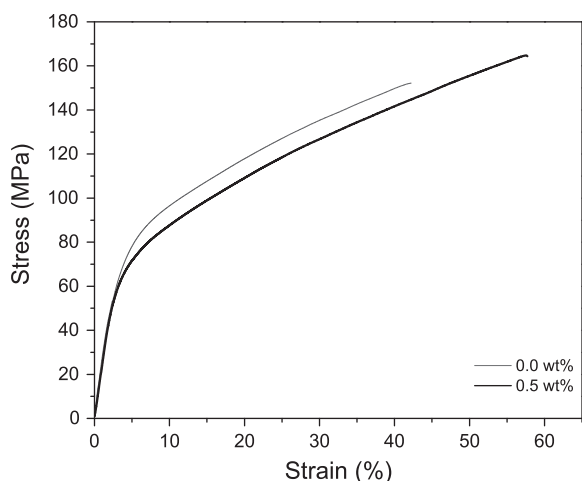


**Fig. 6.** Representative stress–strain curves of the CB/POD nanocomposites.

indicated by the fact that the temperatures ( $T_{d5\%}$ ) at which a 5% weight loss of the POD/CB composites occurred were in the range of 463–468 °C, while the corresponding homopolymer was at 466 °C. The char yields in argon at 700 °C were 59, 57, 57 and 59% to the neat polymer and composites reinforced with 0.1, 0.5 and 1.0 wt.%, respectively. In air,  $T_{d5\%}$ s of polymer and composites were in the range of 463–469 °C with char yield 9%–52% at 700 °C. Surprisingly, the composites with 0.1 wt.% CB show an increase of up to 171% in char yield at 700 °C under air atmosphere. This increase in thermal stability may result from the decrease of free volume and improved adhesion between CB and surrounding POD matrix. Therefore, the observed thermal properties suggest the potential use of this nanocomposites in engineering applications requiring high thermal stability.

### 3.5. Tensile properties of the POD/CB composites

Table 2 lists the tensile properties and Fig. 6 shows the stress–strain curves of neat POD and POD containing 0.1, 0.5 and 1.0 wt.% CB. Young's modulus increased slightly when 0.1 wt.% CB is incorporated into the polyoxadiazole but decrease significantly to the samples with 1.0 wt.% CB. The decrease observed in tensile strength to the samples containing 1.0 wt.% CB implies that possibly in that case aggregates in the POD matrix might act as defect sites, where stress concentration points lower the strength. This result is also well corresponding to the  $\tan \delta$  values discussed previously. The best improvement was observed to the composites reinforced with 0.5 wt.% CB where there was an increase of 5% in tensile strength and 29% in elongation at break (Fig. 6). Such increase reflects in a considerable improvement in the toughness of the composites in relation to the neat polymer. In addition, the decrease in the tensile performance of some of the composites may be attributed to the variation observed in  $M_w$ , Sulfonation level and PDI, which are responsible for a change in the morphology of the composites as well as their structure. The strong interaction between the functionalized CB and the POD matrix greatly enhanced the dispersion as well as the interfacial adhesion, thus strengthening the overall mechanical performance of the composites containing 0.5 wt.% CB.

### 3.6. Morphology of the POD/CB composites

After conducting tensile tests of the POD composites reinforced with 0.5 wt.% CB, the fracture surface was observed by the AFM and TEM to investigate the dispersion state of the CB in the polyoxadiazole matrix. As shown by the AFM images (Fig. 7), the CB formed a core–shell structure, in the order of 50–200 nm, wetted by the polymer [26]. Good distribution could be observed. In accordance with the AFM results, the TEM image (Fig. 8) confirms the homogeneous distribution of the CB aggregates (size of up

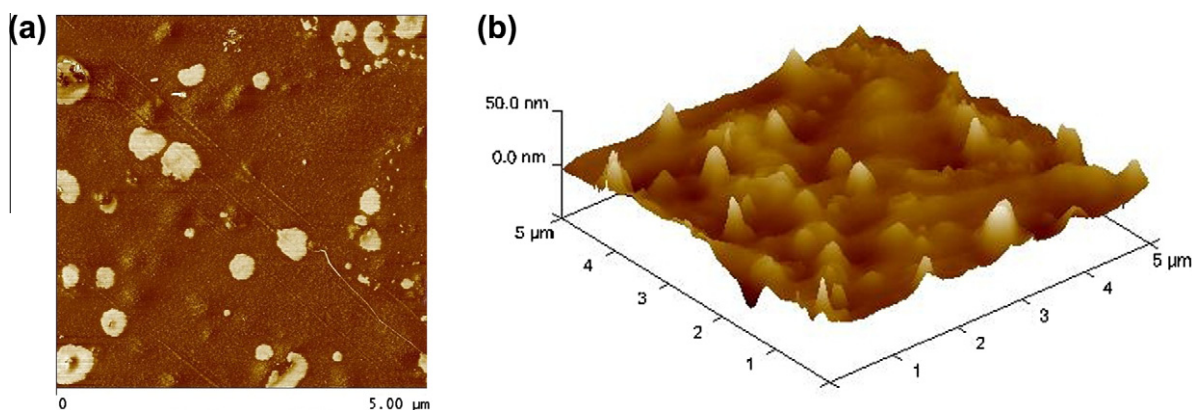


**Fig. 7.** AFM images of the fracture surface of the POD nanocomposites reinforced with 0.5 wt.% of CB after conducting tensile tests.

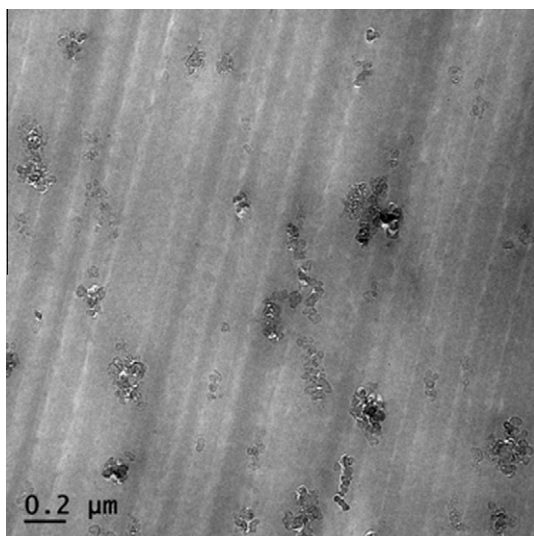


**Fig. 8.** TEM image of the fracture surface of the POD nanocomposites reinforced with 0.5 wt.% of CB after conducting tensile tests.

0.5  $\mu\text{m}$ ) coated by the polyoxadiazole. This might be due to the fact that the carboxyl groups generated on the surface of the CB during the pre-dispersion step effectively anchored the growing of polyoxadiazole chains and improve the interfacial bonding between the CB and the surrounding matrix. The interfacial bonding is expected to enable an effective load transfer between the polymer and filler.

#### 4. Conclusions

In the present work, we demonstrate a fast direct method to obtain POD/CB composites, where the CB is in situ functionalized during the synthesis of poly(1,3,4-oxadiazoles). Sulfonated polyoxadiazole composites containing different concentrations of carbon black (0.1, 0.5 and 1.0 wt.%) were successfully prepared and processed in films using a solution method aided by the use of a mini-calander. The effect of the in situ functionalized CB on the morphological, structural, thermal and mechanical properties of the POD matrix was demonstrated. The presence of CB caused a decrease of up to 15% in the sulfonation level of nanocomposites reinforced with 0.1–0.5 wt.% and an increase of 19% to the composites reinforced with 1.0 wt.%. Composites with high molecular weight ( $10^5$  g/mol) and soluble in polar aprotic solvents were obtained. As a result of the method applied, increase of 31% in storage modulus at 100 °C was observed. The elongation at break shows increases of up to 29% coupled with improvement of tensile strength at low concentration of CB (0.5 wt.%). The increase of  $E'$  observed in the composites with 0.1–0.5 wt.% CB, despite the lower sulfonation level and molecular weight in comparison to the neat POD, was attributed to the homogeneous dispersion and interaction between the CB and the POD. The interaction between the CB and the polyoxadiazole matrix reduce the free volume in the nanocomposites making them behave more elastically. The polyoxadiazole/CB exhibits high thermal stability with degradation temperature at about 460 °C. Composites with 0.1 wt.% CB show an increase of up to 171% in chair yield at 700 °C under air atmosphere. TEM results confirmed the homogeneous dispersion of the CB coated by the polyoxadiazole. This might be due to the fact that the carboxyl groups generated on the surface of the CB during the pre-dispersion step effectively anchored the growing of polyoxadiazole chains and improve the interfacial bonding between the CB and the surrounding matrix. The POD films CB concentration of 0.1 wt.% showed good optical

clarity. The final composites films may be useful candidate for developing new sensor materials, membranes or coatings for high performance applications.

#### Acknowledgements

The authors thank Evonik Degussa GmbH for kindly supply the carbon black used in this work, H. Böttcher for the dynamic mechanical thermal analyses and tensile tests, S. Neumann for the TGA analysis, M. Brinkmann for the SEC measurements, C. Abetz for the TEM images and S. Bolmer for the AFM images. The author M.R. Loos thank Dr. D. Gomes for the previous support.

#### References

- [1] Giannelis EP. Polymer layered silicate nanocomposites. *Adv Mater* 1996;8:29–35.
- [2] Agag T, Koga T, Takeichi T. Studies on thermal and mechanical properties of polyimide–clay nanocomposites. *Polymer* 2001;42:3399–408.
- [3] Jiang X, Bin Y, Matsuo M. Electrical and mechanical properties of polyimide–carbon nanotubes composites fabricated by in situ polymerization. *Polymer* 2005;46:7418–24.
- [4] Hergenrother PM, Jensen BJ, Havens SJ. Poly(arylene ethers). *Polymer* 1988;29:358–69.
- [5] Cornell JW, Hergenrother PM, Wolf P. Chemistry and properties of poly(arylene ether 1,3,4-oxadiazole)s and poly(arylene ether 1,2,4-triazole)s. *Polymer* 1992;33:3507–11.
- [6] Nanjan MJ. Encyclopedia of polymer science and engineering. New York: Wiley; 1987.
- [7] Yang HH. Aromatic high-strength fibers. New York: Wiley; 1989.
- [8] Bach HC, Dobinson F, Lea KR, Saunders JH. High-strength/high-modulus fibers of p-phenylene oxadiazole/n-methyl hydrazide copolymers – a new class of high-performance organic materials. *J Appl Polym Sci* 1979;23:2125–31.
- [9] Cotter RJ, Matzner M. Ring-forming polymerizations. In: Blomquist AF, Wasserman H, editors. Heterocyclic rings, 13B, part B1. New York: Academic Press; 1972.
- [10] Liou GS, Hsiao SH, Chen WC, Yen HJ. A new class of high  $T_g$  and organosoluble aromatic poly(amine-1,3,4-oxadiazole)s containing donor and acceptor moieties for blue-light-emitting materials. *Macromolecules* 2006;39:6036–45.
- [11] Kulkarni AP, Tonzola CJ, Babel A, Jenekhe SA. Electron transport materials for organic light-emitting diodes. *Chem Mater* 2004;16:4556–73.
- [12] Janietz S, Anlauf S. A new class of organosoluble rigid-rod, fully aromatic poly(1,3,4-oxadiazole)s and their solid-state properties, 2a solid-state properties. *Macromol Chem Phys* 2002;203:427–32.
- [13] Gomes D, Roeder J, Ponce ML, Nunes SP. Characterization of partially sulfonated polyoxadiazoles and oxadiazole–triazole copolymers. *J Membr Sci* 2007;295:121–9.
- [14] Gomes D, Roeder J, Ponce ML, Nunes SP. Single-step synthesis of sulfonated polyoxadiazoles and their use as proton conducting membranes. *J Power Sources* 2008;175:49–59.
- [15] Wu TY, Sheu RB, Chen Y. Synthesis and optically acid-sensory and electrochemical properties of novel polyoxadiazole derivatives. *Macromolecules* 2004;37:725–33.
- [16] Yanga NC, Chang S, Suh DH. Synthesis and optically acid-sensory properties of novel polyoxadiazole derivatives. *Polymer* 2003;44:2143–8.
- [17] Kannan B, Gomes D, Dietzel W, Abetz V. Polyoxadiazole-based coating for corrosion protection of magnesium alloy. *Surf Coat Technol* 2008. doi:10.1016/j.surfcoat.2008.03.02.
- [18] Lagrenee M, Mernari B, Chaibi N, Traisnel M, Vezin H, Bentiss F. Investigation of the inhibitive effect of substituted oxadiazoles on the corrosion of mild steel in HCl medium. *Corros Sci* 2001;43:951–62.
- [19] Soutis C. Carbon fiber reinforced plastics in aircraft construction. *Mater Sci Eng A* 2005;412:171–6.
- [20] Meador MA, Campbell SG, Chuang KC, Scheimann DA, Mintz E, Hylton D, Veazie D, Criss J, Kollmansberg R, Tsotsis T. Low-cost, high temperature polymeric materials for space transportation propulsion applications. NASA Technical Reports Server NTRS 2004; Document ID: 20040020118.
- [21] <http://www.key-to-metals.com/Article103.htm>.
- [22] Chuang KC. Low-cost, high glass-transition temperature, thermosetting polyimide developed. NASA Technical Reports Server NTRS 2006; Document ID: 20050187016.
- [23] Wilson D. Polyimide matrix composites: candidates for high speed commercial aircraft or not? *High Perform Polym* 1991;3:73–87.
- [24] Miller S, Papadopoulos D, Heimann P, Inghram L, McCorkle L. Graphite sheet coating for improved thermal oxidative stability of carbon fiber reinforced/PMR-15 composites. *Compos Sci Technol* 2007;66:2183–90.
- [25] Choi J-Y, Han S-W, Huh W-S, Tan L-S, Baek J-B. In situ grafting of carboxylic acid-terminated hyperbranched poly(ether-ketone) to the surface of carbon nanotubes. *Polymer* 2007;48:4034–40.

- [26] Yang Q, Wang L, Xiang W-D, Zhou J-F, Tan Q-H. Preparation of polymer-grafted carbon black nanoparticles by surface-initiated atom transfer radical polymerization. *J Polym Sci Part A* 2007;45:3451–9.
- [27] Shaffer MSP, Fan X, Windle AH. Load transfer in carbon nanotube epoxy composites. *Carbon* 1998;36:1603–12.
- [28] Cai L, Bahr JL, Yao Y, Tour JM. Ozonation of single-walled carbon nanotubes and their assembly on rigid self-assembled monolayers. *Chem Mater* 2002;14:4235–41.
- [29] Mickelson ET, Huffman CB, Rinzler AG, Smalley RE, Hauge RH, Margrave JL. Fluorination of single wall carbon nanotubes. *Chem Phys Lett* 1998;296:188–94.
- [30] Bahr JL, Yang J, Kosynkin DV, Bronikowski MJ, Smalley RE, Tour JM. Functionalization of carbon nanotubes by electrochemical reduction of aryl diazonium salts: a bucky paper electrode. *J Am Chem Soc* 2001;123:6536–42.
- [31] Bahr JL, Tour JM. Highly functionalized carbon nanotubes using in situ generated diazonium compounds. *Chem Mater* 2001;13:3823–4.
- [32] Mitchell CA, Bahr JL, Arepalli S, Tour JM, Krishnamoorti R. Dispersion of carbon nanotubes in polystyrene. *Macromolecules* 2002;35:8825–30.
- [33] Loos MR, Pezzin SH, Amico SC, Bergmann CP, Coelho LAF. The matrix stiffness role on tensile and thermal properties of carbon nanotubes/epoxy composites. *J Mater Sci* 2008;43:6064–9.
- [34] An L, Xu W, Rajagopalan S, Wang C, Wang H, Fan Y. Carbon-nanotube-reinforced polymer-derived ceramic composites. *Adv Mater* 2004;16:2036–40.
- [35] Thostenson ET, Karandikar PG, Chou T-W. Fabrication and characterization of novel reaction bonded carbon nanotube – reinforced ceramic composites. *J Phys D Appl Phys* 2005;38:3962–5.
- [36] Cha SI, Kim KT, Lee KT, Mo CB, Hong SH. Strengthening and toughening of carbon nanotube reinforced alumina nanocomposite fabricated by molecular level mixing process. *Scr Mater* 2005;53:793–7.
- [37] Cha SI, Kim KT, Arshad SN, Mo CB, Hong SH. Extraordinary strengthening effect of carbon nanotubes in metal-matrix nanocomposites processed by molecular-level mixing. *Adv Mater* 2005;17:1377–81.
- [38] Hill DE, Lin Y, Rao AM, Allard LF, Sun YP. Functionalization of carbon nanotubes with polystyrene. *Macromolecules* 2002;35:9466–71.
- [39] Kong H, Gao C, Yan D. Controlled functionalization of multiwalled carbon nanotubes by in situ atom transfer radical polymerization. *J Am Chem Soc* 2004;126:412–3.
- [40] Qu L, Lin Y, Hill DE, Zhou B, Wang W, Sun X. Polyimide-functionalized carbon nanotubes: synthesis and dispersion in nanocomposites films. *Macromolecules* 2004;37:6055–60.
- [41] Ajayan PM. Nanotube from carbon. *Chem Rev* 1999;99:1787–800.
- [42] Smith Jr JG, Connell JW, Delozier DM, Lillehei PT, Watson KA, Lin Y. Space durable polymer/carbon nanotube films for electrostatic charge mitigation. *Polymer* 2004;45:825–36.
- [43] Jin HJ, Choi HJ, Yoon SH, Myung SJ, Shim SE. Carbon nanotube-adsorbed polystyrene and poly(methyl methacrylate) microspheres. *Chem Mater* 2005;17:4034–7.
- [44] Dalton A B, Collins S, Munoz E, Razal JM, Ebron VH, Ferraris JP. Super-tough carbon-nanotube fibres. *Nature* 2003;423:703.
- [45] Gao J, Itkis ME, Yu A, Bekyarova E, Zhao B, Haddon RC. Continuous spinning of a single-walled carbon nanotube-nylon composite fiber. *J Am Chem Soc* 2005;127:3847–54.
- [46] Barraza HJ, Pompeo F, O'Rear EA, Resasco DE. SWNT-filled thermoplastic and elastomeric composites prepared by miniemulsion polymerization. *NanoLetters* 2002;8:797–802.
- [47] Oh SJ, Lee HJ, Keum DK, Lee SW, Wang DH, Park SY, et al. Multiwalled carbon nanotubes and nanofibers grafted with polyetherketones in mild and viscous polymeric acid. *Polymer* 2006;47:1132–40.
- [48] Baek J-B, Lyons CB, Tan LS. Grafting of vapor-grown carbon nanofibers via in-situ polycondensation of 3-phenoxybenzoic acid in polyphosphoric acid. *Macromolecules* 2004;37:8278–85.
- [49] Wang DH, Mirau P, Li B, Li CY, Baek J-B, Tan LS. Solubilization of carbon nanofibers with a covalently attached hyperbranched poly(ether-ketone). *Chem Mater* 2008;20:1502–15.
- [50] Eo S-M, Oh S-J, Tan L-S, Baek J-B. Poly(2,5-benzoxazole)/carbon nanotube composites via in-situ polymerization of 3-amino-4-hydroxybenzoic acid hydrochloride in a mild poly(phosphoric acid). *Eur Polym J* 2008;44:1603–12.
- [51] Loos MR, Gomes D. The effect of sulfonation level and molecular weight on the tensile properties of polyoxadiazoles. *High Perform Polym* 2009;21:697–708.
- [52] Gomes D, Loos MR, Wichmann MHG, de la Vega A, Schulte K. Sulfonated polyoxadiazole composites containing carbon nanotubes prepared via in-situ polymerization. *Compos Sci Technol* 2009;69:220–7.
- [53] Jäger C, Henning Th, Schlögl R, Spillecke O. Spectral properties of carbon black. *J Non-Cryst Solids* 1999;258:161–79.
- [54] Siemann U. Solvent cast technology – a versatile tool for thin film production. *Progr Colloid Polym Sci* 2005;130:1–14.
- [55] Toshio O, Yuichi I, Takashi I. Properties of vapor grown carbon nano fiber/phenylethynyl terminated polyimide composite. *Adv Compos Mater* 2004;13:215–26.
- [56] Chou W-J, Wang C-C, Chen C-Y. Characteristics of polyimide-based nanocomposites containing plasma-modified multi-walled carbon nanotubes. *Compos Sci Technol* 2008;68:2208–13.
- [57] Cho D-H, Lee S-Y, Yang G-G, Fukushima H, Drzal LT. Dynamic mechanical and thermal properties of phenylethynyl-terminated polyimide composites reinforced with expanded graphite nanoplatelets. *Macromol Mater Eng* 2005;209:179–87.
- [58] Hsueh H-B, Chen C-Y. Preparation and properties of LDHs/polyimide nanocomposites. *Polymer* 2003;44:1151–61.
- [59] Muhammad K, Shaikat S, Zahoor AJ. Properties of binary polyimide blends containing hexafluoroisopropylidene group. *Macro Sci Part A* 2007;44:55–63.